High Power Laser Science and Engineering, (2024), Vol. 12, e41, 5 pages.
doi:10.1017/hpl.2024.22

HIGH POWER LASER SCIENCE AND ENGINEERING

RESEARCH ARTICLE

High-efficiency tandem Ho:YAG single-crystal fiber laser delivering more than 100 W output power

Jianlei Wang[1], Zihao Tong[2], Changsheng Zheng[2], Tianyi Du[2], Yongguang Zhao[2], and Chun Wang[1]

[1] *Key Laboratory of Laser & Infrared System, Ministry of Education, Shandong University, Qingdao, China*

[2] *Jiangsu Collaborative Innovation Center of Advanced Laser Technology and Emerging Industry, Jiangsu Normal University, Xuzhou, China*

(Received 20 February 2024; revised 3 April 2024; accepted 17 April 2024)

Abstract

We report on a high-efficiency, high-power tandem Ho:YAG single-crystal fiber (SCF) laser in-band pumped by a Tm-doped fiber laser at 1907 nm. In addition to the uniform heat distribution resulting from the large surface-to-volume ratio of this fiber-like thin-crystal rod, the long gain region provided by the tandem layout of two SCFs enables high lasing efficiency and power handling capability. More than 100 W output power is achieved at 2.1 μm, corresponding to a slope efficiency of 70.5% and an optical-to-optical efficiency of 67.6%. To the best of our knowledge, this is the highest output power and efficiency ever reported from SCF lasers in the 2-μm spectral range.

Keywords: high efficiency; Ho:YAG; power handling capability; single-crystal fiber

1. Introduction

High-power solid-state lasers in the 2-μm spectral range have been widely applied in various fields, including remote sensing, lidar, laser surgery and therapy, laser welding of transparent plastics and pumping mid-infrared (mid-IR) optical parametric oscillators (OPOs) for mid-IR frequency conversion[1–4]. Tm^{3+}-doped, Ho^{3+}-doped gain media provide the main approach to directly generate 2-μm high-power lasers[5,6]. Compared to the Tm^{3+} ions, the large emission cross-section of Ho^{3+} ions doped crystals makes them more suitable to achieve high power 2-μm lasers; for instance, yttrium aluminum garnet ($Y_3Al_5O_{12}$, YAG) crystals doped with Ho^{3+} ions have a gain cross-section seven times larger than that of Tm:YAG[7,8].

Figure 1 presents an overview of continuous-wave (CW) Ho lasers in the 2-μm spectral range[8–26], containing Ho:YAG bulk, thin-disk, slab and Ho:fiber laser systems, illustrating the significant advances in terms of high power and efficiency that have been achieved in recent years. Currently, YAG is still the preferred host material for high-power laser operation due to its high thermal conductivity, mechanical robustness, ease-of-preparation and excellent chemical properties[27]. Nevertheless, further power scaling of Ho:YAG lasers remains challenging and needs to be combined with different strategies for high power generation, for example, high doping concentrations of Ho^{3+} ions[13], cryogenically cooled systems[9,10], single gain medium or dual gain media in conjunction with dual-end-pumping schemes[13,15–17,19,20,22,23], wing pumping systems[21] and gain media with end caps[20] or in special structures (i.e., the slab[9,10,19] or thin-disk geometry[12,18]). By comparison, current concepts for power scaling of 2-μm laser sources are inclined to use Tm-[28] or Ho-doped silica fibers[23–26] due to their simple thermal management, high brightness and compact structure; however, the nonlinear effects, optical damage, photon darkening and transverse mode instability (TMI)[29,30] in fiber lasers seriously limit further power scaling.

Alternatively, the optical fiber structure in combination with the crystal properties of YAG offers an effective approach for achieving high average/peak power.

Correspondence to: Y. Zhao, Jiangsu Collaborative Innovation Center of Advanced Laser Technology and Emerging Industry, Jiangsu Normal University, Xuzhou 221116, China. Email: yongguangzhao@yeah.net; C. Wang, Key Laboratory of Laser & Infrared System, Ministry of Education, Shandong University, Qingdao 266237, China. Email: chunwang@sdu.edu.cn

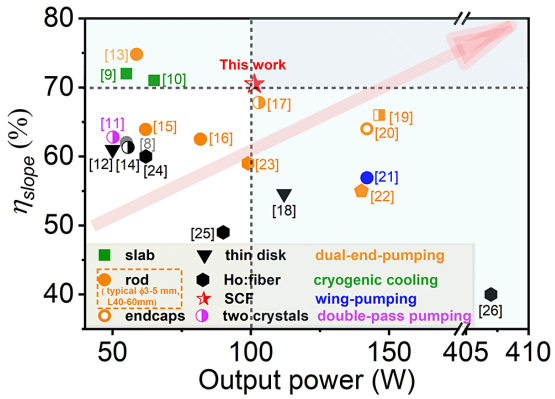

Figure 1. Overview of 2-μm continuous-wave (CW) Ho:YAG and Ho:fiber lasers[8–26].

Theoretically, the critical power supported by YAG single-crystalline fibers is six times higher than that of traditional silica fibers[31,32]. Note that the concept of single-crystal fiber (SCF) is somewhat misleading but already established, referring to fiber-like thin-crystal rods with a large surface-to-volume ratio and characterized by a diameter of less than 1 mm and a length of a few centimeters. Some reports in the 1-μm spectral region, for example, a 250 W CW laser from a compact resonant cavity[33] and an average power of 290 W with 829 fs pulses in a two-stage amplifier[34] based on Yb-doped YAG SCFs[35,36], all indicate that SCFs are ideal gain media for high average/peak power laser oscillators/amplifiers.

However, there have been relatively few studies on high-power SCF lasers in the 2-μm spectral range to date. Most recently, we have reported on the wing-pumped Tm:YAG SCF laser delivering 63 W output power at 2.01 μm[37]. In terms of lasers based on Ho:YAG SCFs, the Ho:YAG SCF fabricated by the laser heated pedestal growth (LHPG) method was reported for the first time at 2.09 μm, and a quasi-CW output power of 23.5 W was achieved under pulsed pumping (10 Hz repetition rate, 50% duty cycle), while an output power roll-off at 10 W was observed due to thermal issues under CW pumping[38]. The CW output power of 35.2 W was achieved from an oscillator based on a YAG SCF doped with 0.6% (atomic fraction) Ho^{3+} ions grown by the micro-pulling-down (μ-PD) method[39], while the corresponding slope efficiency was less than 45% and the thermal effect was obvious at approximately 30 W laser power. Thus, the unique geometry structure of SCFs with large surface-to-volume ratio and the latest progress of SCF oscillators in the 2-μm spectral region motivated us to study the power scaling capability of CW SCF lasers, aiming to obtain high-power lasers.

In this paper, the CW laser performance of the tandem Ho:YAG SCF was investigated in a compact resonator with a 1907 nm Tm-doped fiber laser (TDFL) as the pump source. Benefiting from the high brightness of the in-band pumping scheme and the tandem-set SCFs with fiber-like geometry structure, a maximum output power of 101.3 W with a slope efficiency of 70.5% was achieved at the pump power of 153 W. To the best of our knowledge, this is the highest power and efficiency of Ho:YAG SCF lasers, which proves the power scalability of SCF lasers and paves the way towards SCF ultrafast amplifiers emitting at 2 μm directly.

2. Experimental details

The experimental setup of the tandem Ho:YAG SCF laser with a physical cavity length of approximately 105 mm is depicted in Figure 2. A 1907-nm TDFL with a good beam quality of M^2 ~ 1.1 was used as the pump source. The pump beam passed through a telescope system, and then was focused into the latter part of the first SCF with

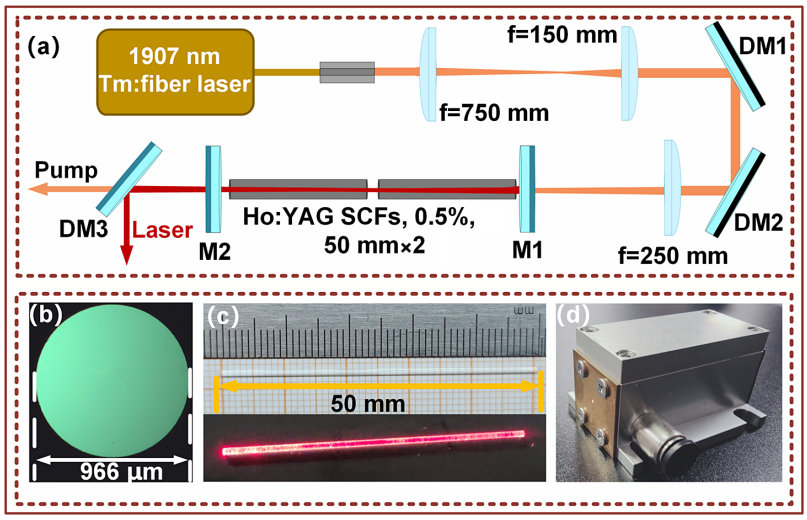

Figure 2. Experimental setup of the tandem Ho:YAG SCF laser.

a spot diameter of approximately 520 μm. Two series-arranged 0.5% (atomic fraction) Ho^{3+}-doped YAG SCFs (966 μm in diameter and 50 mm in length) were employed as gain media, as shown in Figures 2(b) and 2(c), which were mechanically fabricated by cutting and grounding the Czochralski-grown Ho:YAG crystals. All the entire lateral surfaces and end facets of the SCFs were optically polished, and all end facets of SCFs were anti-reflection (AR) coated at 1.9 and 2.1 μm, which can avoid parasitic laser oscillations and etalon effects. Figure 2(b) displays a photograph of the end facet of the Ho:YAG SCF. The transmission losses of Ho:YAG SCFs were measured to be less than 3 dBm^{-1} at 632.8 nm. The mirror M1 was flat with high reflectivity at 2.1 μm and high transmission at 1.9 μm. The flat mirrors M2 with different transmissions (T_{OC} = 30%, 50%, 70% and 90%) for the laser wavelength were used as output couplers (OCs). A dichroic mirror (DM3) was used to separate the laser and pump beams. To mitigate the thermal load, all SCFs were mounted on a specially designed water-cooled aluminum heat sink with both ends glue-sealed, which were directly water-cooled to 8°C, as shown in Figure 2(d).

3. Results and discussion

Figure 3(a) shows the output power as a function of the incident pump power with different transmissions of T_{OC} = 30%, 50%, 70% and 90%. The most efficient operation was achieved with T_{OC} = 70% OC; a maximum output power of 101.3 W was achieved at the incident pump power of 153 W (~97.7% pump absorption ratio under lasing conditions), corresponding to a slope efficiency of 70.5% and an optical conversion efficiency of 67.6% at the maximum output power. Compared to the reported complex Ho:YAG (Ho ions doping concentration of 0.8% atomic fraction) dual-crystal folded cavity where each crystal is double-ended pumped by Tm:YLF lasers[17], a more compact scheme (single-end pumped dual-SCFs) was utilized to achieve higher slope efficiency (>70%) in this work. The CW output power of 65 W was obtained with the OC of T_{OC} = 30%, and the slope efficiency was decreased to 69%, which may be caused by the high-power density and the thermal effect at the low OC transmission. Output powers and slope efficiencies with high-transmission OCs (T_{OC} = 50%, 70% and 90%) are higher compared to our previous report[39], which is attributed to the longer gain region, the spatial uniform distribution of pump intensity and the large overlap between the pump and laser beams in the directly water-cooled tandem SCFs, thus resulting in high slope efficiencies of more than 70% and 100-W-level output powers.

The measured optical spectra of the tandem Ho:YAG SCF laser with different OCs are depicted in Figure 3(b) and the gain spectra of Ho:YAG[40] are also shown for easy comparison. Two emission peaks for high-transmission OCs may be

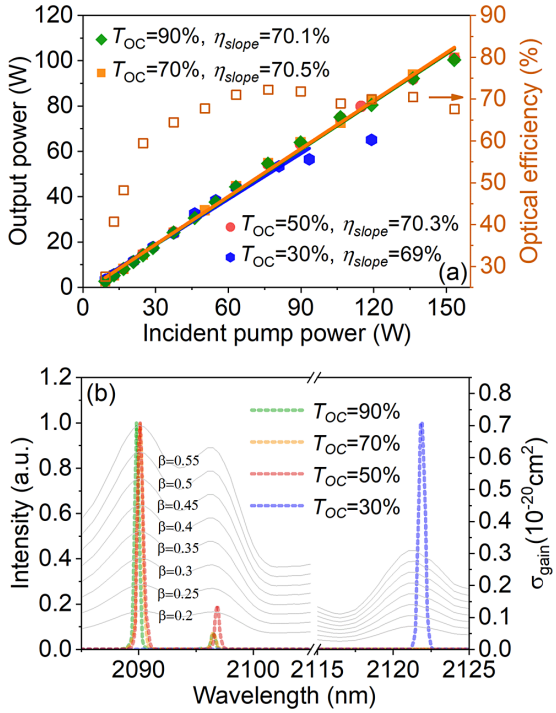

Figure 3. (a) CW laser output powers and (b) the corresponding optical spectra of the Ho:YAG tandem SCF laser with different OC transmissions (T_{OC} = 30%, 50%, 70% and 90%).

caused by the same gain cross-sections. The wavelength of the laser emission operated from approximately 2090 nm to 2121 nm with decreasing transmittance of the OC, and such a wavelength red shift of approximately 31 nm is a typical feature of the quasi-three-level system due to the stronger reabsorption effect as there is lower population inversion with the low transmission of the OC[39].

By evaluating the round-trip resonator loss of the tandem Ho:YAG SCF laser, the modified Caird analysis was used as a commonly adapted method to plot the inverse of the slope efficiencies versus the inverse of the OC reflections. The losses and the intrinsic slope efficiency of the laser can be estimated by the following[41]:

$$1/\eta_S = 1/\eta_0\,(1+2\gamma/\gamma_{OC}),$$

$$\gamma = -\ln(1-L),$$

$$\gamma_{OC} = -\ln(1-T_{OC}),$$

where η_S is the measured slope efficiency, η_0 is the intrinsic slope efficiency, L is the internal loss per pass, γ_{OC} is the output-coupling loss and T_{OC} is the transmission of the OC. As shown in Figure 4, the linear relationship between the experimentally measured points of the inverse slope efficiency ($1/\eta_S$) as a function of OC reflections ($-1/\ln(R_{OC})$) provides a straightforward way to determine the internal loss per pass (L) and intrinsic slope efficiency (η_0).

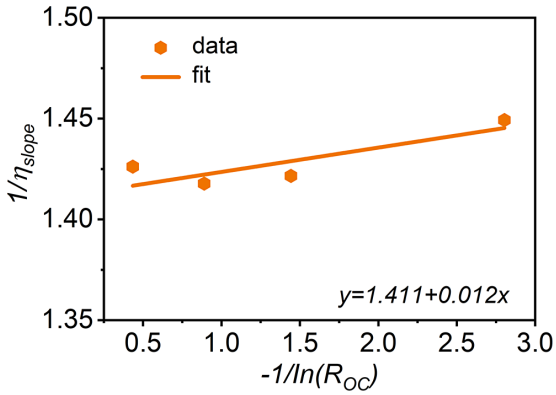

Figure 4. Caird plot for the tandem Ho:YAG SCF laser: inverse slope efficiency with respect to the inverse output-coupling loss.

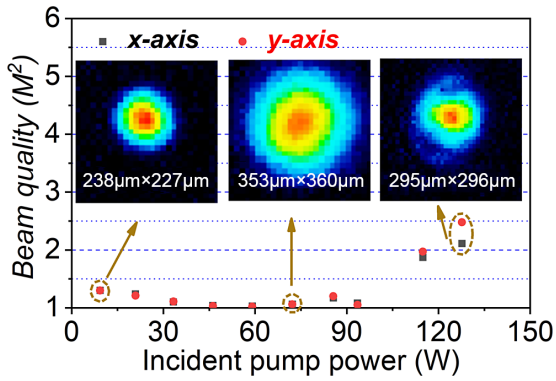

Figure 5. The measured beam quality at different power levels; the insert is the corresponding near-field beam profiles.

The best fit value of the propagation loss was determined to be $L/l = 0.0004$ cm^{-1}, and the intrinsic slope efficiency was calculated to be approximately 70.9%, which is very nearly equal to the measured slope efficiency, indicating the great potential of the designed laser for further power scaling and future ultrashort-pulse SCF amplification experiments.

The beam propagation factors (M^2) of the tandem Ho:YAG SCF laser with $T_{OC} = 70\%$ were recorded to assess the beam quality with a mid-IR charge-coupled device (CCD) camera (WinCamD-IR-BB, Dataray, Inc.) at different pump powers. The similar trend of the beam propagation factors along the x- and y-axes indicates that tandem-set SCFs provide a uniform heat distribution in their transverse cross-section. As shown in Figure 5, when the incident pump power was less than 100 W, the M^2 factors measured in both the x- and y-directions were around 1.1 by taking advantage of the large surface-to-volume ratio of the SCF and the direct water-cooling scheme. However, the excitation of higher-order transverse modes gradually degrades the beam quality at the pump power of approximately 130 W, resulting in M^2 factors along the x- and y-directions of 2.11 and 2.48, respectively. The beam quality along the y-axis deteriorates more seriously than that along the x-axis, which may be caused by unidirectional heat dissipation of the approximately 1 mm protuberance of the SCF outside the module under high pump power levels. Further beam propagation factor optimization and power improvement can be realized by employing SCFs with diffusion-bonded undoped YAG end caps, or optimizing the directly water-cooled aluminum heat sink without protuberances of SCFs outside the module, thus mitigating thermal effects under high pump power levels.

4. Conclusion

In summary, we have experimentally investigated the laser performance of tandem-set Ho:YAG SCFs. The maximum output power of more than 100 W was obtained with a slope efficiency of more than 70% by taking advantage of the long gain region, the large surface-to-volume ratio and the low propagation loss of SCFs. Compared to our previous work[39], we simply reduced the doping concentration of Ho^{3+} ions in the YAG SCF and employed two directly water-cooled tandem SCFs as the gain medium to reduce the thermal effect and extend the gain length, thus resulting in high-power, high-efficiency laser output. Such a high-performance laser based on the tandem-set SCFs demonstrates an efficient way to realize high-power output and lays the foundation for expanding the output power of SCF lasers to a few hundred watts in the near future. Furthermore, the tandem-set SCFs not only provide a long gain region and simple thermal management due to their fiber-like geometry and crystal properties, but also suppress nonlinear effects and nonlinear phase accumulation effectively, thus paving the way for high average/peak power femtosecond pulse amplification.

Acknowledgement

This work was supported by the National Natural Science Foundation of China (Nos. 62075090 and 52032009).

References

1. S. W. Henderson, C. P. Hale, J. R. Magee, M. J. Kavaya, and A. V. Huffaker, Opt. Lett. **16**, 773 (1991).
2. T. Sumiyoshi, H. Sekita, T. Arai, S. Sato, M. Ishihara, and M. Kikuchi, IEEE J. Sel. Top. Quantum Electron. **5**, 936 (1999).
3. A. Dergachev, D. Armstrong, A. Smith, T. Drake, and M. Dubois, Opt. Express **15**, 14404 (2007).
4. I. Mingareev, F. Weirauch, A. Olowinsky, L. Shah, P. Kadwani, and M. Richardson, Opt. Laser Technol. **44**, 2095 (2012).
5. A. Godard, C. R. Phys. **8**, 1100 (2007).
6. B. M. Walsh, Laser Phys. **19**, 855 (2009).
7. K. Scholle, S. Lamrini, P. Koopmann, and P. Fuhrberg, in *Frontiers in Guided Wave Optics and Optoelectronics* (IntechOpen, 2010), p. 471.
8. S. Lamrini, P. Koopmann, M. Schäfer, K. Scholle, and P. Fuhrberg, Appl. Phys. B **106**, 315 (2012).

9. M. Ganija, A. Hemming, N. Simakov, K. Boyd, N. Carmody, P. Veitch, J. Haub, and J. Munch, Appl. Phys. B **126**, 72 (2020).
10. M. Ganija, A. Hemming, N. Simakov, K. Boyd, J. Haub, P. Veitch, and J. Munch, Opt. Express **25**, 31889 (2017).
11. B. Yao, Y. Shen, X. Duan, W. Wang, Y. Ju, and Y. Wang, J. Russ. Laser Res. **34**, 503 (2013).
12. J. Zhang, F. Schulze, K. Mak, V. Pervak, D. Bauer, D. Sutter, and O. Pronin, Laser Photonics Rev. **12**, 1700273 (2018).
13. Y. Shen, B. Yao, X. Duan, T. Dai, Y. Ju, and Y. Wang, Appl. Opt. **51**, 7887 (2012).
14. F. Chen, M. Cai, Y. Zhang, and B. Li, Proc. SPIE **11023**, 110233P (2019).
15. B. Yao, Y. Shen, L. Han, C. Qian, X. Duan, Y. Ju, and Y. Wang, Opt. Quant. Electron **47**, 211 (2015).
16. S. Mi, J. Tang, D. Wei, B. Yao, J. Li, K. Yang, T. Dai, and X. Duan, Opt. Express **30**, 21501 (2022).
17. Y. Shen, B. Yao, X. Duan, G. Zhu, W. Wang, Y. Ju, and Y. Wang, Opt. Lett. **37**, 3558 (2012).
18. S. Tomilov, M. Hoffmann, Y. Wang, and C. J. Saraceno, J. Phys. Photonics **3**, 022002 (2021).
19. X. Duan, Y. Shen, B. Yao, and Y. Wang, Quantum Electron. **48**, 691 (2018).
20. M. Ganija, A. Hemming, K. Boyd, A. Gambell, and N. Simakov, in *CLEO Pacific Rim* (Optica Publishing Group, 2020), paper C9A_2.
21. W. Yao, E. Li, Y. Shen, C. Ren, Y. Zhao, D. Tang, and D. Shen, Laser Phys. Lett. **16**, 115001 (2019).
22. A. Hemming, S. Bennetts, N. Simakov, A. Davidson, J. Haub, and A. Carter, Opt. Express **21**, 4560 (2013).
23. A. Hemming, S. Bennetts, N. Simakov, A. Davidson, J. Haub, and A. Carter, in *Advanced Photonics*, OSA Technical Digest (CD) (Optica Publishing Group, 2011), paper SOMB1.
24. B. Beaumont, P. Bourdon, A. Barnini, L. Kervella, T. Robin, and J. L. Gouët, J. Lightwave. Technol. **40**, 6480 (2022).
25. J. Gouët, F. Gustave, P. Bourdon, T. Robin, A. Laurent, and B. Cadier, Opt. Express **28**, 22307 (2020).
26. A. Hemming, N. Simakov, A. Davidson, S. Bennetts, M. Hughes, N. Carmody, P. Davies, L. Corena, D. Stepanov, J. Haub, R. Swain, and A. Carter, in *CLEO: 2013*, OSA Technical Digest (online) (Optica Publishing Group, 2013), paper CW1M.1.
27. I. F. Elder, and M. J. P. Payne, Opt. Commun. **148**, 265 (1998).
28. W. Yao, C. Shen, Z. Shao, J. Wang, F. Wang, Y. Zhao, and D. Shen, Appl. Opt. **57**, 5574 (2018).
29. M. N. Zervas and C. A. Codemard, IEEE J. Sel. Top. Quantum Electron. **20**, 0904123 (2014).
30. C. Jauregui, C. Stihler, and J. Limpert, Adv. Opt. Photonics **12**, 429 (2020).
31. L. Dong, J. Ballato, and J. Kolis, Opt. Express **31**, 6690 (2023).
32. T. Parthasarathy, R. Hay, G. Fair, and F. Hopkins, Opt. Eng. **49**, 094302 (2010).
33. X. Délen, S. Piehler, J. Didierjean, N. Aubry, A. Voss, M. A. Ahmed, T. Graf, F. Balembois, and P. Georges, Opt. Lett. **37**, 2898 (2012).
34. F. Beirow, M. Eckerle, T. Graf, and M. A. Ahmed, Appl. Phys. B **126**, 148 (2020).
35. Y. Zhao, C. Zheng, Z. Huang, Q. Gao, J. Dong, K. Tian, Z. Yang, W. Chen, and V. Petrov, Laser Photonics Rev. **16**, 2200503 (2022).
36. C. Zheng, T. Du, L. Zhu, Z. Wang, K. Tian, Y. Zhao, Z. Yang, H. Yu, and V. Petrov, Photonics Res. **12**, 27 (2024).
37. J. Wang, J. Dong, J. Liu, Z. Wang, X. Xu, Y. Xue, J. Xu, C. Wang, and Y. Zhao, Opt. Express **30**, 29015 (2022).
38. Y. Li, K. Miller, E. G. Johnson, C. D. Nie, S. Bera, J. A. Harrington, and R. Shori, Opt. Express **24**, 9751 (2016).
39. Y. Zhao, L. Wang, W. Chen, J. Wang, Q. Song, X. Xu, Y. Liu, D. Shen, J. Xu, X. Mateos, P. Loiko, Z. Wang, X. Xu, U. Griebner, and V. Petrov, High Power Laser Sci. Eng. **8**, e25 (2020).
40. Y. Wang, R. Lan, X. Mateos, J. Li, C. Hu, C. Li, S. Suomalainen, A. Harkonen, M. Guina, V. Petrov, and U. Griebner, Opt. Express **24**, 18003 (2016).
41. J. Morris, N. K. Stevenson, H. T. Bookey, A. K. Kar, C. T. A. Brown, J. M. Hopkins, M. D. Dawson, and A. A. Lagatsky, Opt. Express **25**, 14910 (2017).